Journal of COMPUTATIONAL CHEMISTRY

Could an Anisotropic Molecular Mechanics/Dynamics Potential Account for Sigma Hole Effects in the Complexes of Halogenated Compounds?

Krystel El Hage,[a,b] Jean-Philip Piquemal,[c] Zeina Hobaika,[b] Richard G. Maroun,[b] and Nohad Gresh*[a]

Halogenated compounds are gaining an increasing importance in medicinal chemistry and materials science. Ab initio quantum chemistry (QC) has unraveled the existence of a "sigma hole" along the C—X (X = F, Cl, Br, I) bond, namely, a depletion of electronic density prolonging the bond, concomitant with a build-up on its sides, both of which are enhanced along the F < Cl < Br < I series. We have evaluated whether these features were intrinsically built-in in an anisotropic, polarizable molecular mechanics (APMM) procedure such as SIBFA (sum of interactions between fragments ab initio computed). For that purpose, we have computed the interaction energies of fluoro-, chloro-, and bromobenzene with two probes: a divalent cation, Mg(II), and water approaching X through either one H or its O atom. This was done by parallel QC energy-decomposition analyses (EDA) and SIBFA computations. With both probes, the leading QC contribution responsible for the existence of the sigma hole is the Coulomb contribution E_c. For all three halogenated compounds, and with both probes, the in- and out-of-plane angular features of E_c were closely mirrored by the SIBFA electrostatic multipolar contribution (E_{MTP}). Resorting to such a contribution thus dispenses with empirically-fitted "extra", off-centered partial atomic charges as in classical molecular mechanics/dynamics. © 2013 Wiley Periodicals, Inc.

DOI: 10.1002/jcc.23242

Introduction

Halogenated compounds constitute about 35% of the drugs in current use in medicinal chemistry.[1–3] The onset of ligand–protein or ligand–nucleic "halogen bonding" is highlighted by numerous X-ray crystallographic studies.[4–6] Halogen bonding is also frequently encountered in materials and supramolecular chemistry.[7] An understanding of the electronic effects resulting from selective halogenation could very significantly contribute to optimizing both the affinities and the selectivities of ligands to their targets, and to fine-tune recognition processes in supramolecular complexes. Earlier QC studies quantified directionality effects in a diversity of complexes of ligands having C—X bonds (X = F, Cl, Br, and I) with O—containing biological sites from the Protein Data Bank.[4] A remarkable feature of halogenated compounds is the existence of a "sigma-hole", namely, a depletion of electronic density prolonging the C—X bond, concomitant with a build-up on its sides.[8] Both effects are enhanced along the F < Cl < Br < I series.[8a] The binding of electron-rich ligands to the CX bonds of a series of halogenated derivatives were the object of recent high-level QC studies including energy-decomposition analyses.[9] Regarding halobenzenes, and in order to account for such an effect in classical molecular dynamics, a fictitious atom is added prolonging the C—X bond. For each halobenzene, it is endowed with a partial charge, an equilibrium distance to X bearer, and stretching and bending constants which are all fit.[10] This additional center enabled for improved agreements with respect to QC intermolecular interaction energies as well as for improved Molecular Dynamics and Monte-Carlo simulations. Recent examples[10] reported comparisons with MP2 calculations for the approach of O— and N— containing probes along the C—X bond, although directionality effects were not reported. In our laboratories, we are applying an anisotropic, polarizable molecular mechanics/dynamics procedure, SIBFA,[11] to study the complexes of drugs with several protein targets such as kinases[12] and metalloproteins.[13] Thus, the far-reaching impact of selective halogenations on the binding affinities is a strong incentive to incorporate halogenated derivatives in our library of compounds. It was critical to evaluate if both sigma-hole effects and binding anisotropies were inherently built-in in the procedure without the need for extraneous fictitious charges. For that purpose, we have analyzed by parallel ab initio QC and SIBFA computations the binding energies of three halobenzenes (X = F—, Cl—, and Br) with two probes. The first is a divalent cation, Mg(II), used deliberately in order to magnify the amplitudes of electrostatic effects of the sigma

---

[a] *K. E. Hage, N. Gresh*
Laboratoire de Chimie Biochimie Pharmacologiques et Toxicologiques, UMR 8601 CNRS, UFR Biomédicale, Paris, France
E-mail: nohad.gresh@parisdescartes.fr

[b] *K. E. Hage, Z. Hobaika, R. G. Maroun*
Unité de Biochimie, Université Saint-Joseph, Beirut, Lebanon

[c] *J.-P. Piquemal*
Laboratoire de Chimie Théorique, UMR7616 CNRS, UPMC, Paris, France

Contract/grant sponsor: GENCI (CINES/IDRIS); Contract/grant numbers: 2009-075009; Contract/grant sponsor: Centre de Ressources Informatiques de Haute Normandie (CRIHAN, Rouen, France); Contract/grant number: 1998053.

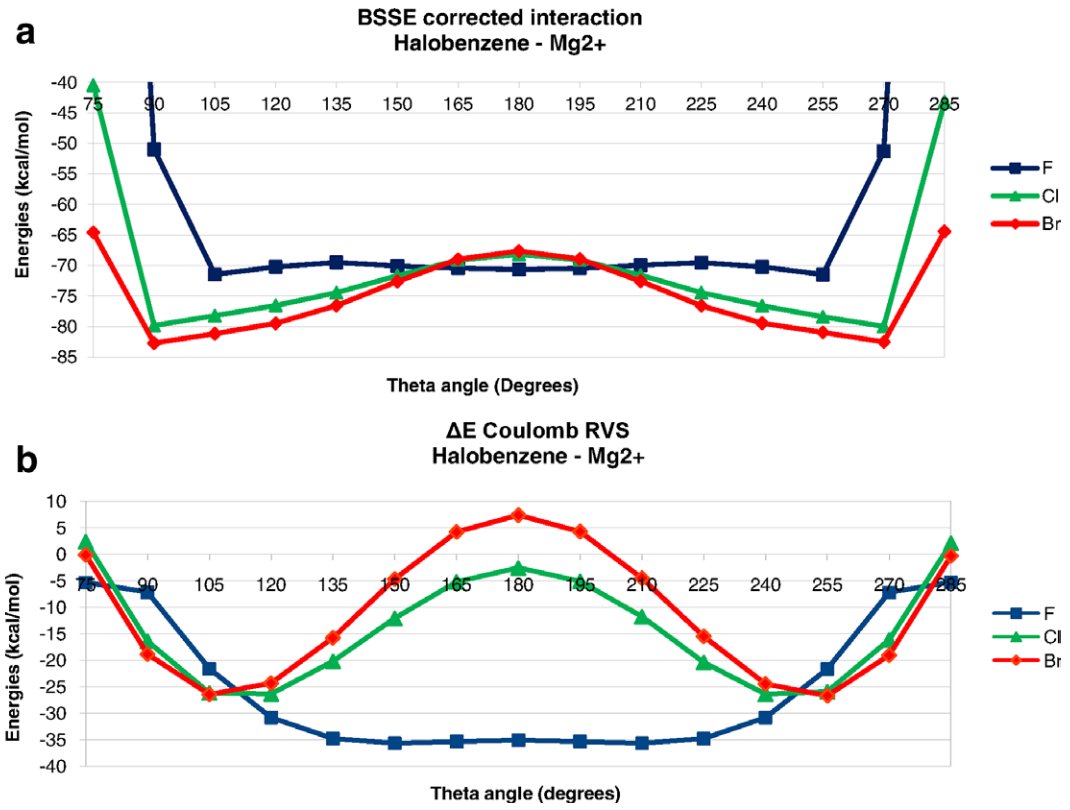

Figure 1. a–b). Halobenzene–Mg(II) complex. In-plane evolutions of a) ΔE(RVS) and b) E_C, as a function of the θ angle.

hole. The second is water, approaching either along one H, or along its O atom. The X-to probe (P = Mg(II), H, or O) distance R is first optimized for an approach with a θ angle (C—X—P) of 180°. We then investigate the effects of in-plane θ variations at optimized distance R, followed by out-of-plane variations at optimized θ and R. Such angular variations probe electron depletion along the C—X bonds and its anisotropic build-up upon varying the θ and ϕ (C—C—X—P) angles, and how well the QC interaction energies can be matched by the SIBFA ones. In this article, we will essentially focus on the electrostatic contribution, which was shown from previous studies[9] to be the leading contribution conferring angularity to ΔE(QC) in the energy-meaningful range of θ values.

Procedure

The QC calculations were done with the aug-ccpVTZ(-f) basis set.[14] The pseudopotential containing basis set, aug-ccpVTZ-PP(-f), was used to describe bromine. This pseudopotential implicitly describes relativistic effects, which for large atoms, such as bromine, play an important role to describe their electronic properties.[15] EDA analyses were done with the Reduced Variational Space Analysis (RVS)[16] using the GAMESS package.[17] ΔE(RVS) is decomposed into the first-order Coulomb (E_c) and exchange-repulsion (E_{exch}) and second-order polarization (E_{pol}) and charge-transfer (E_{ct}). Probing the effects of correlation and dispersion will be reported in a subsequent study. In the SIBFA computations, the energy is computed as a sum of five contributions: electrostatic multipolar (E_{MTP}), short-range repulsion (E_{rep}), polarization (E_{pol}), charge-transfer (E_{ct}), and dispersion (E_{disp}). E_{MTP} resorts to distributed atomic charges, dipoles, and quadrupoles. They were derived for each halobenzene and for water from their QC wave function as computed with the Gaussian package[18] and using the Stone analysis.[19] The quadrupoles were converted from the spherical to the Cartesian representation. For compatibility with the SIBFA software, each quadrupolar tensor was then reformulated under the form of two quadrupoles with intensities and normalized principal axes, according to the original formulation of Claverie and coworkers.[20] This was done by a home-built routine (Mike Devereux, Paris, 2010). E_{pol} is computed with distributed polarizabilities distributed on the bond barycenters and the lone pair heteroatoms, using the procedure by Garmer and Stevens[21] in the GAMESS package. The parameters for F, Cl, and Br were calibrated so that ΔE(SIBFA) matches ΔE(RVS) upon Mg(II) approach along the CX bond and the corresponding equilibrium distances to within 0.1 Å. Details will be provided in a forthcoming paper. It has to be noted that while separability of E_{pol} and E_{ct} in second-order is a distinctive feature of the SIBFA procedure, their relative weights within the second-order contribution can be affected by the size of the basis set as well as of the level of theory, namely upon passing from noncorrelated to correlated calculations.[22] The NCI (noncovalent interactions) plots were drawn using the procedure reported in Ref. [23], which is co-developed in one of our laboratories.

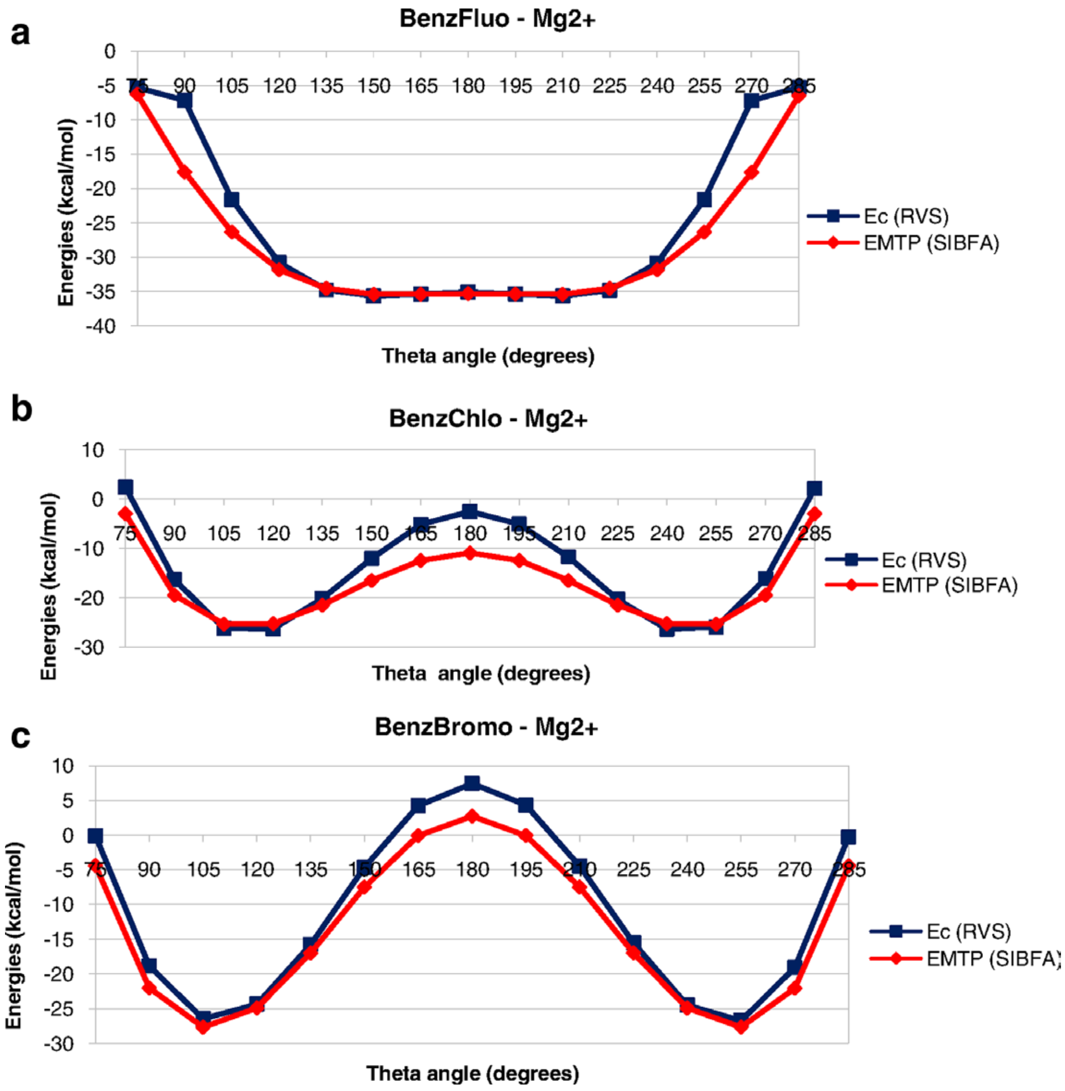

Figure 2. a–c) Halobenzene–Mg(II) complex. Compared in-plane evolutions of E_C and of E_{MTP} as a function of the θ angle for a) fluorobenzene, b) chlorobenzene, and c) bromobenzene.

Results and Discussion

Mg(II) probe

The optimized QC X–Mg(II) distances for $\theta = 180°$ are 1.8, 2.2, and 2.3 Å, for F, Cl, and Br, respectively.

In-plane angular variations Figures 1a and 1b display the evolutions of ΔE(RVS) and of its E_C contribution, respectively, for in-plane variations of θ at these distances. For fluorobenzene, both ΔE(RVS) and E_C have a flat behavior in the 120–240° range. By contrast, for both chloro- and bromobenzene, ΔE(RVS) and E_C display marked anisotropies with a maximum at $\theta = 180°$. Comparison of Figures 1a and 1b shows that for both compounds in the range 135–225°, the angularity of ΔE(RVS) is mirrored by that of E_C. In the 135–105° and 225–255° intervals, their decreases are slower but remain comparable, namely about 5 and 10 kcal/mol for chloro- and bromobenzene, respectively. For both compounds, E_C has symmetric minima at 105° and 255° while ΔE(RVS) has its minima shifted by 15°, namely at 90° and 270°. This is due to E_{pol} favoring increasingly shorter distances between the probe and either CH bond *ortho* to the CX bond, but counteracted by E_{rep}. While for all three halobenzenes, E_{pol} decreases sharply for $\theta < 90°$ and $> 270°$, this is compensated by concomitant sharp rises in E_{rep} with E_{ct} flat in the whole 75–285° range (unpublished). For $\theta < 90°$ and $\theta > 270°$, steric clashes occur with the CH bonds, and these angular values are thus irrelevant.

The corresponding evolutions of E_{MTP} for the three halobenzenes are given in Figures 2a–2c. For each halobenzene, and for more clarity, we display again the corresponding E_C evolutions. For all three compounds, there is a striking superimposition of the E_{MTP} and E_C curves. Thus, similar to E_C, E_{MTP} has a flat behavior for fluorobenzene in the 135–225° range, translating the absence of sigma-hole. E_{MTP} has a definite maximum at 180° for both chloro- and bromobenzene, and minima at 105–120° for chlorobenzene and at 105° for bromobenzene. These are exactly the same features as for E_C, translating the depletion of electron density prolonging the CCl and CBr

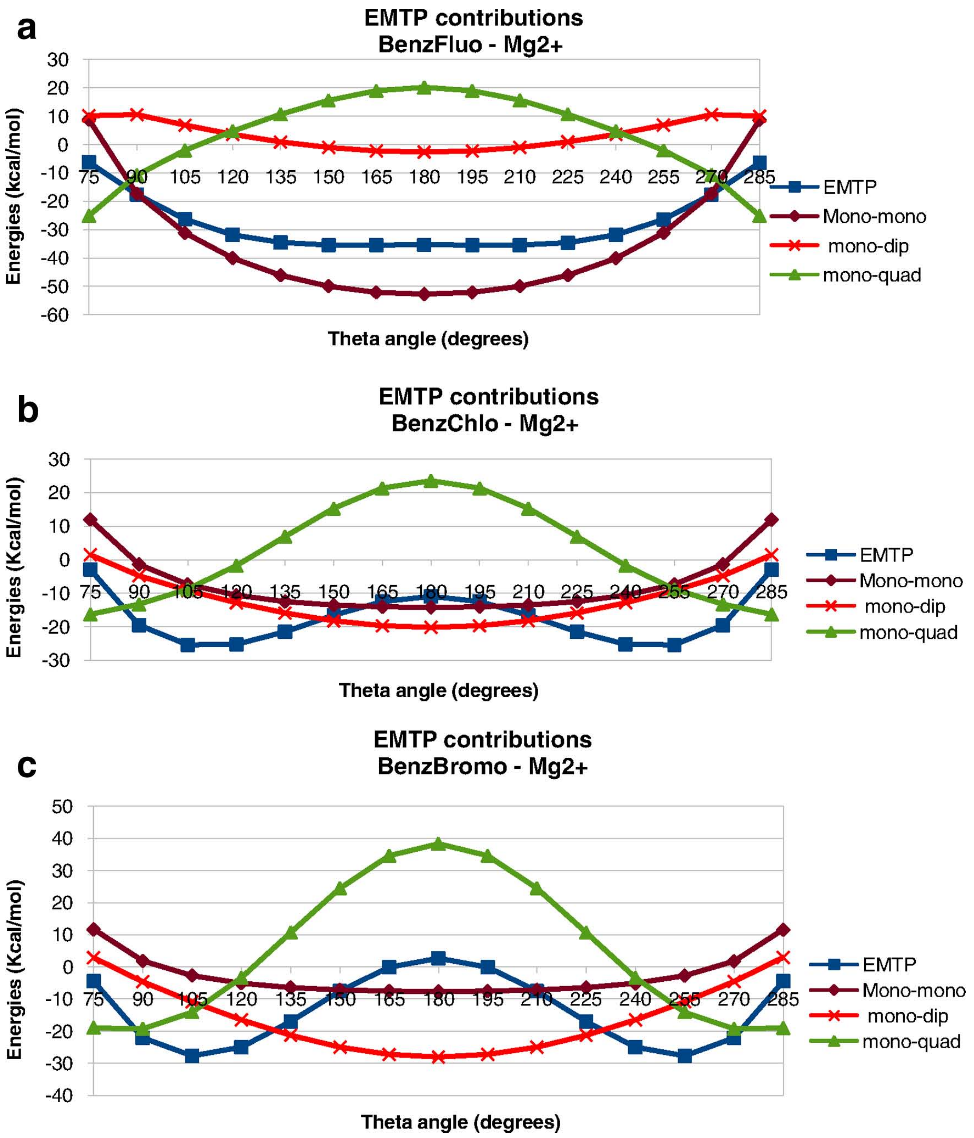

Figure 3. a–c) Halobenzene–Mg(II) complex. In-plane evolutions of E_{MTP} and its components as a function of the θ angle for a) fluorobenzene, b) chlorobenzene, and c) bromobenzene. [Color figure can be viewed in the online issue, which is available at wileyonlinelibrary.com.]

bonds, and its build-up on their sides. For all three halobenzenes, the numerical values of E_{MTP} are very close to those of E_C except in the 150–210° and 165–195° ranges for chloro- and bromobenzene, respectively, where E_C is the least attractive for an electron-deficient probe. These results demonstrate that the effects of the sigma hole on the QC Coulomb contribution can be inherently and closely accounted for by E_{MTP}, without any need for extraneous fictitious charges as in classical molecular mechanics/dynamics. It also appears that resorting to higher-order multipoles than quadrupoles may not be necessary, except possibly for θ in the range 150–210° where electron depletion is maximal.

In order to trace back the origin of E_{MTP} in-plane angular preferences, we display in Figures 3a–3c the angular evolutions of the separate charge–charge, charge–dipole, and charge–quadrupole components. In the fluorobenzene complex, the flat behavior of E_{MTP} is seen to result from very strong mutual compensations between charge–charge, favoring $\theta = 180°$ on the one hand, and charge–quadrupole, favoring $\theta = 90°$ and $\theta = 270°$ on the other hand. Thus, in order to account for the *isotropic* behavior of the Coulomb contribution in this complex, a nonisotropic molecular mechanics electrostatic contribution is needed. A related situation could be recalled from the earliest implementation of another contribution, charge transfer, in SIBFA.[24] The flat behavior of E_{ct} in the linear water dimer upon performing out-of-plane displacement of the electron-acceptor water monomer was found to result from mutual compensations between the individual contributions to E_{ct} of each of the two lone pairs of the electron-donating water monomer. The increase of E_{ct} contributed by one lone pair which occurred upon progressively aligning the OH acceptor bond along its direction was compensated by the concomitant decrease of E_{ct} contributed by the other lone pair. Here, upon passing to the chloro- and the bromobenzene complexes, the charge–charge term becomes less and less attractive and increasingly shallower. The charge–dipole term

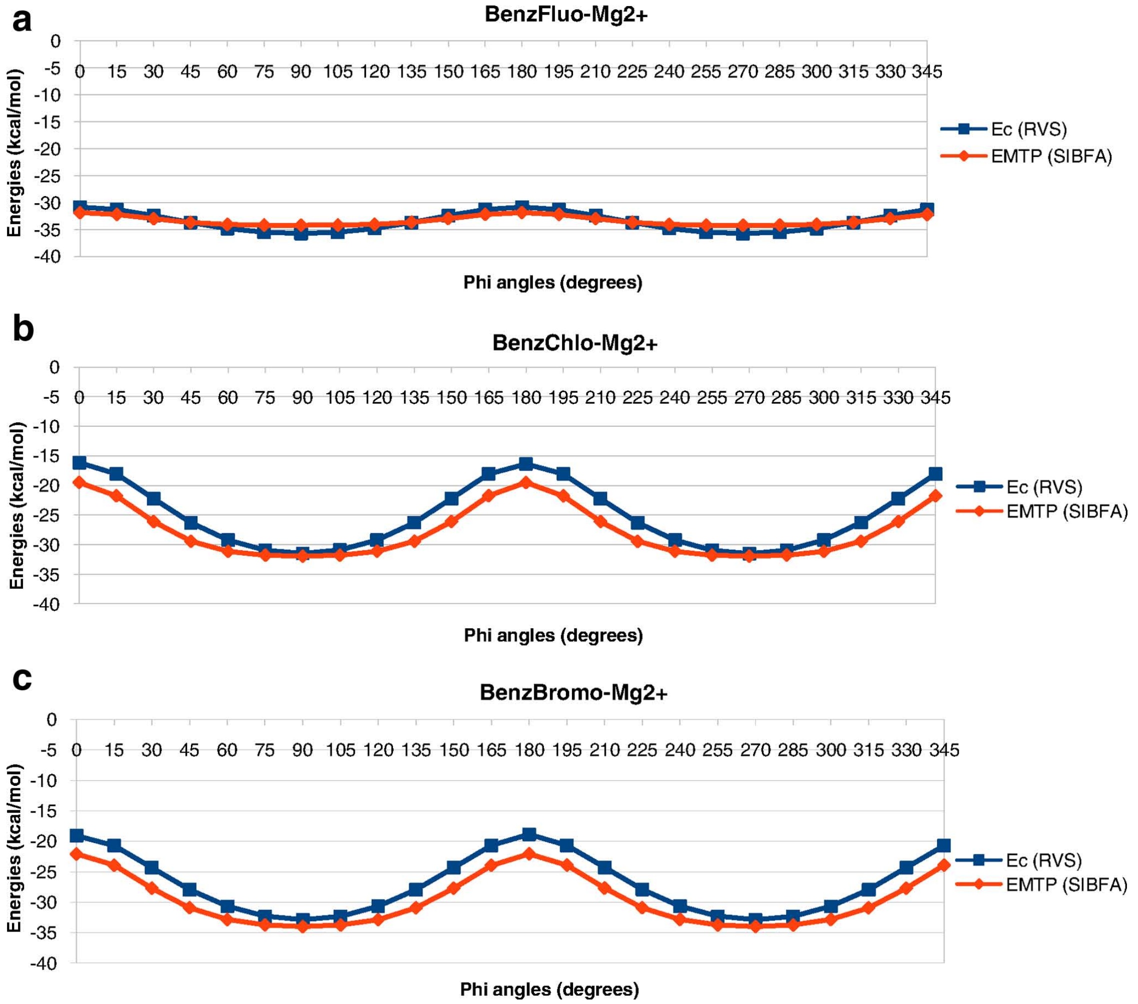

Figure 4. a–c) Halobenzene–Mg(II) complex. Compared out-of-plane evolutions of E_C and of E_{MTP} as a function of the ϕ angle for a) fluorobenzene, b) chlorobenzene, and c) bromobenzene. [Color figure can be viewed in the online issue, which is available at wileyonlinelibrary.com.]

becomes increasingly attractive and favors θ =180°. By contrast, the charge–quadrupole term becomes increasingly repulsive toward $\theta = 180°$ and increasingly attractive toward $\theta = 90°$ and 270°. While the relative weights of these different terms in E_{MTP} could differ according to the different procedures to derive multipoles from molecular orbitals, the present analysis appears fully consistent with chemical intuition.

Out-of-plane angular variations We have in a second step performed out-of-plane variations of the probe upon stepwise variation of the ϕ angle C—C—X—Mg, the values of the θ angles being set at 105° for fluorobenzene and at 90° for chloro- and bromobenzene, which correspond to their values optimizing ΔE(RVS). Figures 4a–4c report the evolutions of E_c and E_{MTP} for the three halobenzenes, and Figures 5a–5c those of the separate E_{MTP} components. E_{MTP} closely parallels the evolutions of E_c throughout. For fluorobenzene, both E_c and E_{MTP} are shallow. For chloro- and bromobenzene, the in-plane positions are the least favorable, and the optimized ϕ values are in the ranges 60–105° and 255–300°, about 10 kcal/mol more favorable than at $\phi = 180°$ or 0°. This implies that upon optimizing the binding of chloro- and bromobenzene to electron-deficient ligands, out-of-plane approaches could be significantly more favored than in-plane approaches. This is in marked contrast with the binding of electron-rich ligands, for which the approach toward the sigma hole is along the CX direction with an optimal θ of 180°, namely in-plane. Also in contrast with the in-plane variations, the angular behaviors are for both chloro- and bromobenzene now dictated by charge–charge, while charge–quadrupole favors the in-plane positions with $\phi = 0°$ and 180° and charge–dipole is flat. This could not stem from the sole reduction in the electrostatic repulsion between Mg(II) and either CH bond ortho to the CX bond, occurring upon rotating Mg(II) out of the halobenzene plane, as it is the Mg(II)–fluorobenzene complex having the shortest (1.8 Å) Mg–X distance for which the charge–charge term undergoes the least variations amongst halobenzenes.

The use of Mg(II) as a probe for the sigma hole can be further illustrated by NCI plots taken at the θ different values (Figure 6). Thus (Fig. 6a), the contours between fluorobenzene and the probe change color upon passing from $\theta = 90°$ to $\theta = 180°$, namely from red (unfavorable) to green to pale blue, translating the increasing strength of the interaction. These

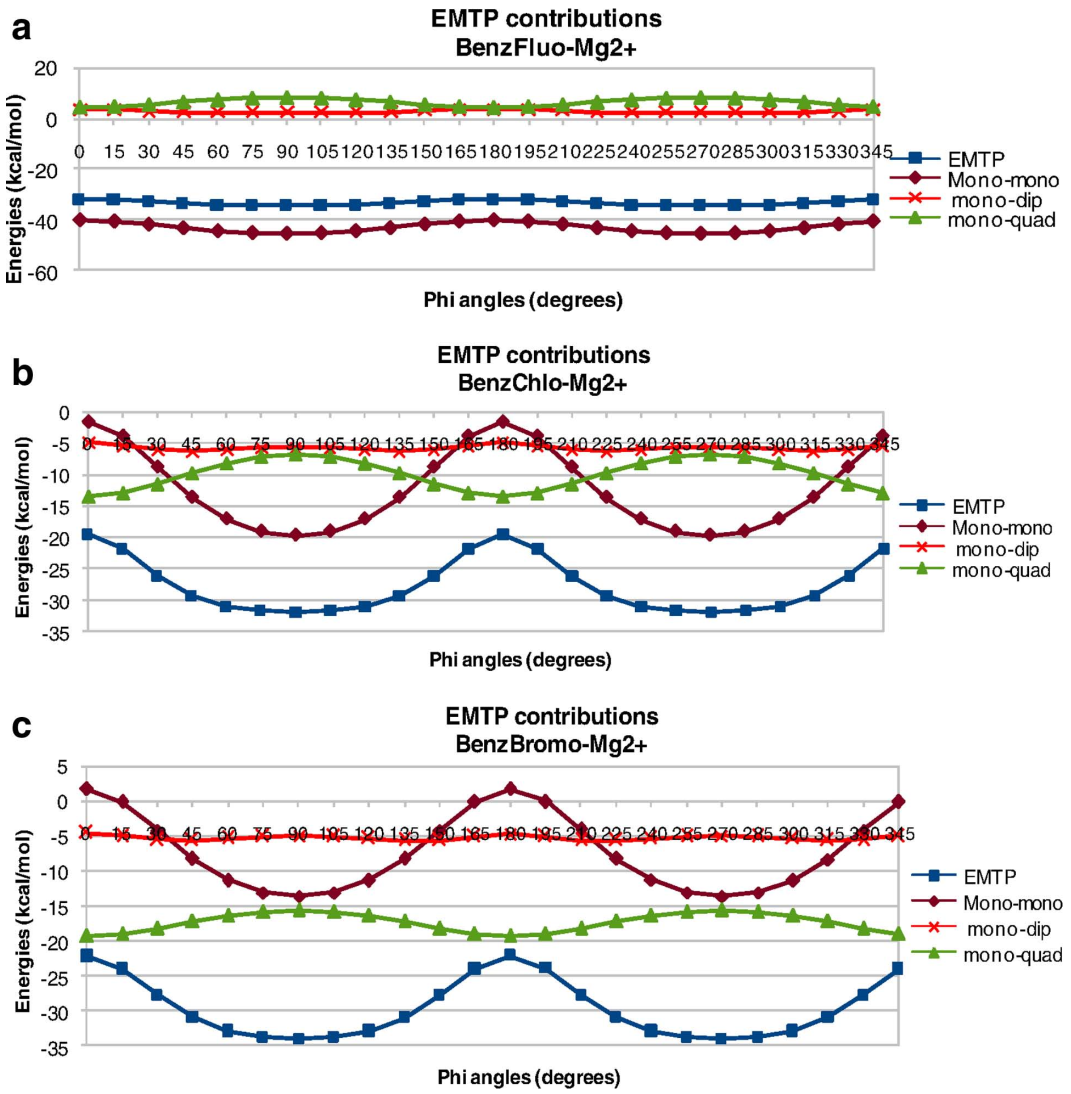

Figure 5. a–c) Halobenzene–Mg(II) complex. Out-of-plane evolutions of E_{MTP} and its components as a function of the ϕ angle for a) fluorobenzene, b) chlorobenzene, and c) bromobenzene. [Color figure can be viewed in the online issue, which is available at wileyonlinelibrary.com.]

evolutions parallel those of ΔE(RVS) and E_C(RVS). The reverse trends are found for chloro- and bromobenzene. For chlorobenzene (Fig. 6b), the intensity of the blue contours increases upon decreasing θ from 180° to 120°, where E_C reaches its minimum. An additional green contour appears at 105° and 90°, translating the onset of an additional, weaker attractive interaction with a CH bond and a CC bond ortho to the CCl one, explaining why ΔE(RVS) reaches its minimum at a smaller θ value (90°) than E_C (120°). For the smallest θ value (75°), the appearance of an orange contour translates the onset of a repulsive interaction between the probe and the CCl and that CC bond. Very similar trends are found with bromobenzene (Fig. 6c), the minima of ΔE(RVS) and of E_C now being much closer (90° and 105°, respectively). The intensities of the contours translate those of the total energies, not just those of their sole Coulomb contributions. Thus, while the Mg(II) complex of fluorobenzene at $\theta = 180°$ has a more E_C favorable value than the chloro- and bromobenzene complexes at $\theta = 120°$ and 105°, respectively, its corresponding contour has a lesser intensity, due to an actually lesser ΔE(RVS) owing to a weaker polarization energy.

Water probe

The distances of approach to the halogen were optimized using the B3LYP procedure augmented with a dispersion energy term,[25] and denoted as B97D.

Approach through one H atom The three halobenzenes were probed by water approaching the CX bond through one H atom, the CX—HO bonds being collinear, the second OH bond being perpendicular to the halobenzene plane. The optimized ΔE(B97D) values are at H···X distances of 2.3, 2.6, and 2.7 Å, for X = F, Cl, and Br, respectively. For all three complexes, the angular features of both ΔE(RVS) and E_C(RVS) are similar to those found with the corresponding Mg(II) complexes (Figures 7a and 7b), but their amplitudes of variations, contained within 3 kcal/mol, are now considerably reduced. Figures 8a–8c show that again the variations of E_{MTP} can match those of E_C

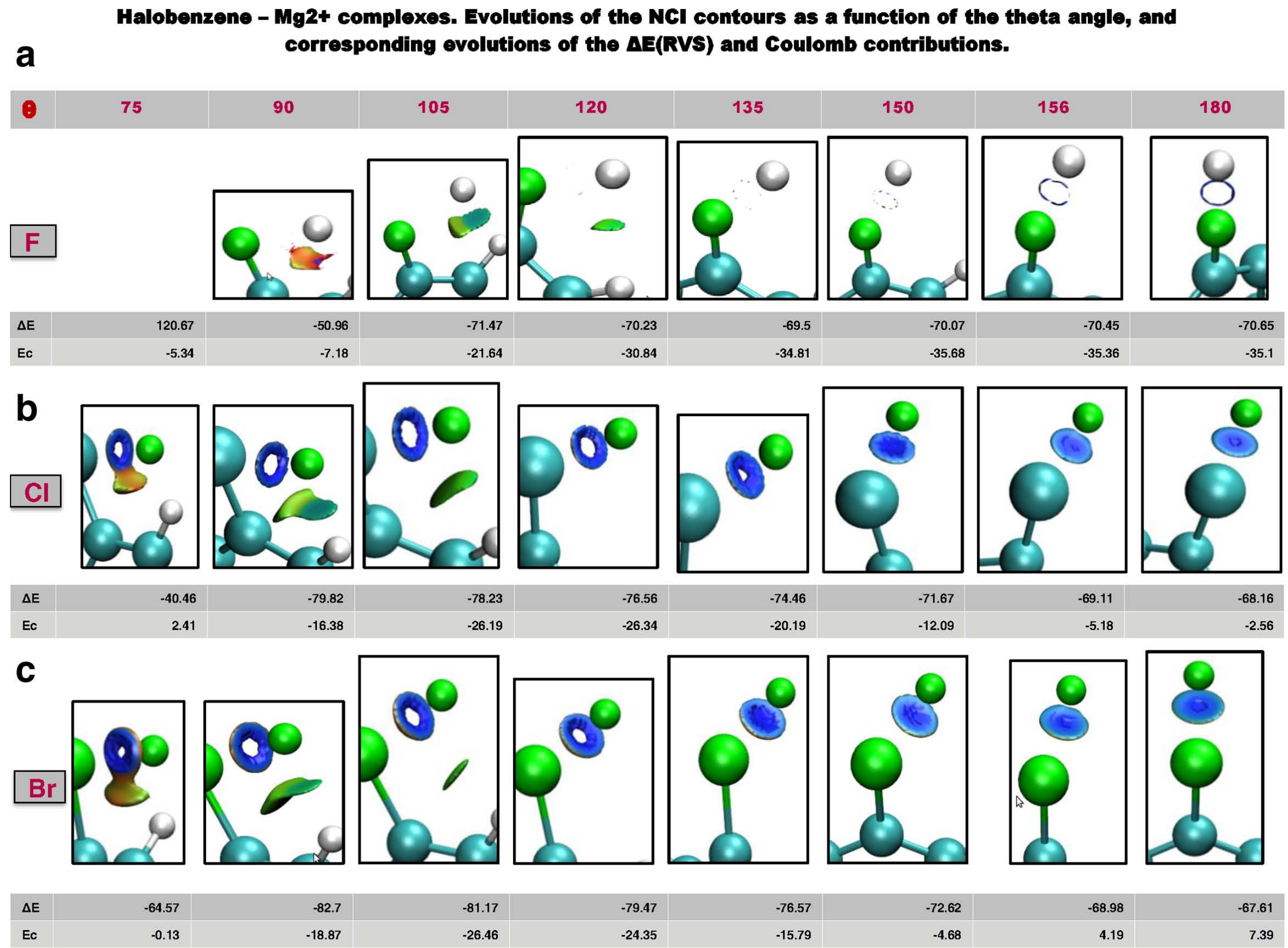

Halobenzene – Mg2+ complexes. Evolutions of the NCI contours as a function of the theta angle, and corresponding evolutions of the ΔE(RVS) and Coulomb contributions.

a

θ	75	90	105	120	135	150	156	180
ΔE	120.67	-50.96	-71.47	-70.23	-69.5	-70.07	-70.45	-70.65
Ec	-5.34	-7.18	-21.64	-30.84	-34.81	-35.68	-35.36	-35.1

b

θ	75	90	105	120	135	150	156	180
ΔE	-40.46	-79.82	-78.23	-76.56	-74.46	-71.67	-69.11	-68.16
Ec	2.41	-16.38	-26.19	-26.34	-20.19	-12.09	-5.18	-2.56

c

θ	75	90	105	120	135	150	156	180
ΔE	-64.57	-82.7	-81.17	-79.47	-76.57	-72.62	-68.98	-67.61
Ec	-0.13	-18.87	-26.46	-24.35	-15.79	-4.68	4.19	7.39

Figure 6. a–c). Halobenzene–Mg(II) complex. NCI plots at successive in-plane variations of the θ angle. a) Fluorobenzene, b) chlorobenzene, and c) bromobenzene. [Color figure can be viewed in the online issue, which is available at wileyonlinelibrary.com.]

variations over the whole range of energy relevant θ values, namely 90–270°.

Approach through the O atom The three halobenzenes were probed by water approaching the CX bond through its O atom. The optimized ΔE(B97D) values are at O···X distances of 3.1 Å for X = Cl and Br. No stable complex was found with fluorobenzene, and this investigation was thus limited to chloro- and bromobenzene. Figures 9a and 9b display the in-plane θ variations of ΔE(RVS) and E_C, respectively. For both halobenzenes, the energy minima now occur at $\theta = 180°$. In the absence of correlation/dispersion, ΔE(RVS) is found to be slightly repulsive. The E_C minimum also occurs at $\theta = 180°$. It is more attractive for bromobenzene than chlorobenzene (−1.7 vs. −0.6 kcal/mol, respectively). E_C has lesser amplitudes of variations than ΔE(RVS), owing to steep variations of E_{exch} as water approaches either CH bond ortho to the CX one, as illustrated in Figure 8c. For both halobenzene complexes, E_{MTP} and E_{rep}(SIBFA) can match to within 0.5 kcal/mol the in-plane angular behaviors of their RVS counterparts. This is illustrated in Figures 10a and 10b regarding E_{MTP}, in Figures 9c and 9d regarding E_{rep}, and in Figures 10e and 10f regarding the total energies.

The induction of σ-holes by an incoming partial negative charge was recently shown to contribute to the stability of hydrogen bonding.[26] This finding led us to consider if a related effect was at play with the σ-holes of halogenated compounds. In the context of SIBFA, we have thus compared the magnitudes of the halobenzene polarization energies in their complexes with water. In the 135–225° range, and for the bromobenzene complex, E_{pol} has about 1.5 larger magnitudes for water approaching through its O atom than through one of its H atoms (−0.5 vs. −0.3 kcal/mol, respectively). The ratio was smaller (1.2) in the chlorobenzene complex. These results are in line with those of Ref. [26], and also indicate a greater σ-hole sensitivity to a partially negative charge of bromo- than chlorobenzene.

Conclusions and Perspectives

The present results demonstrate that the impact of a sigma hole in halobenzenes can be successfully accounted for by an anisotropic polarizable molecular mechanics procedure, SIBFA. This is enabled by the computation of the electrostatic contribution, E_{MTP}, which resorts to distributed ab initio QC multipoles. We have first probed the electron-rich regions of

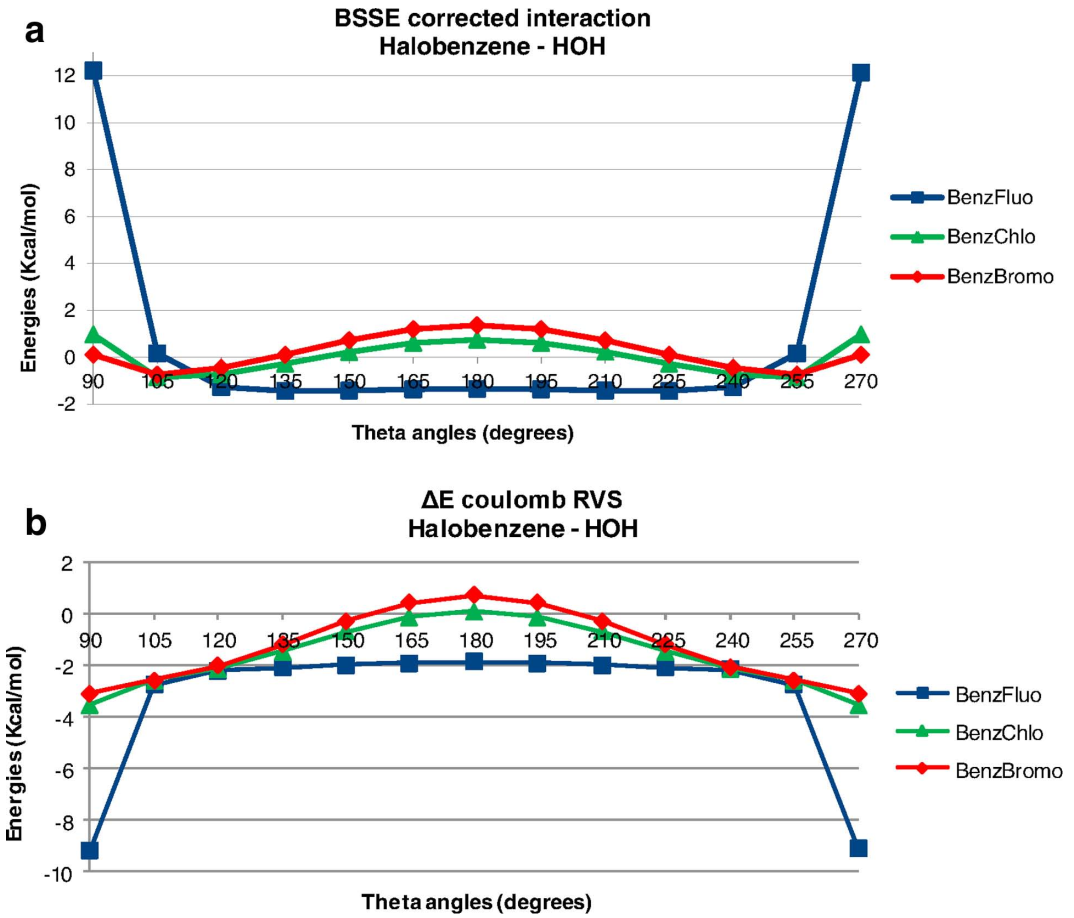

Figure 7. a–b) Halobenzene–water complex. Water approach through one H atom. In-plane evolutions of a) ΔE(RVS) and b) E_C, as a function of the θ angle. [Color figure can be viewed in the online issue, which is available at wileyonlinelibrary.com.]

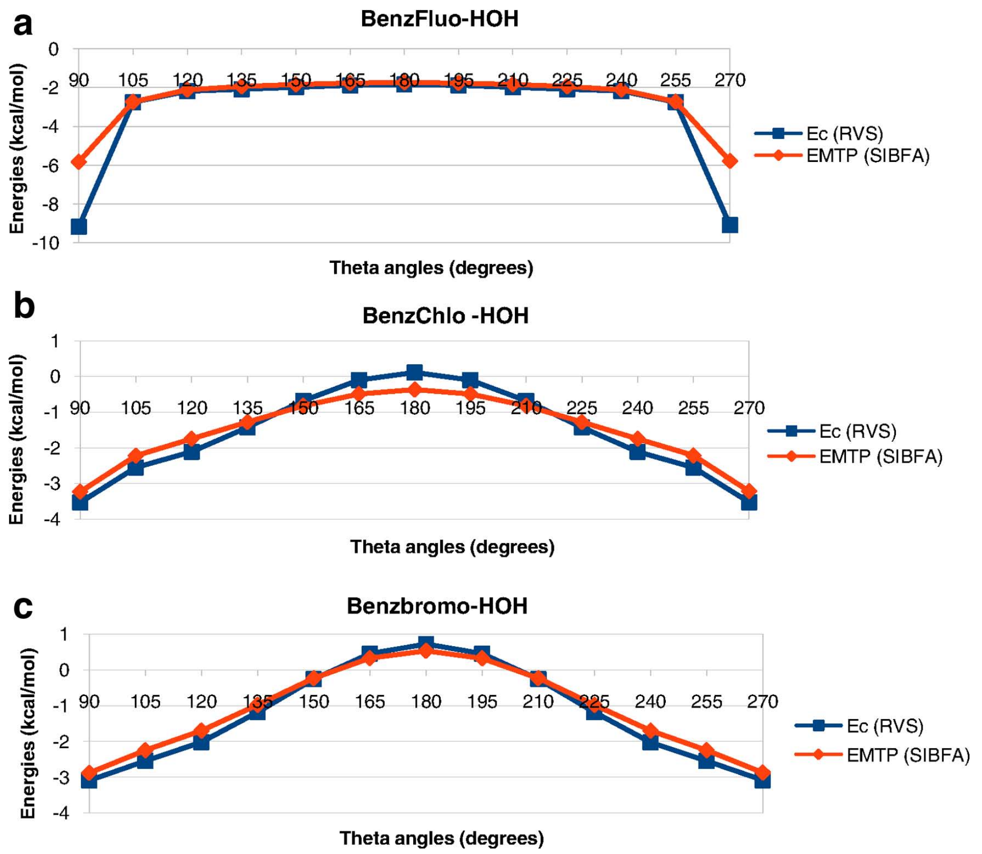

Figure 8. a–c) Halobenzene–water complex. Water approach through one H atom. Compared in-plane evolution E_C and E_{MTP} as a function of the θ angle for a) fluorobenzene, b) chlorobenzene, and c) bromobenzene. [Color figure can be viewed in the online issue, which is available at wileyonlinelibrary.com.]

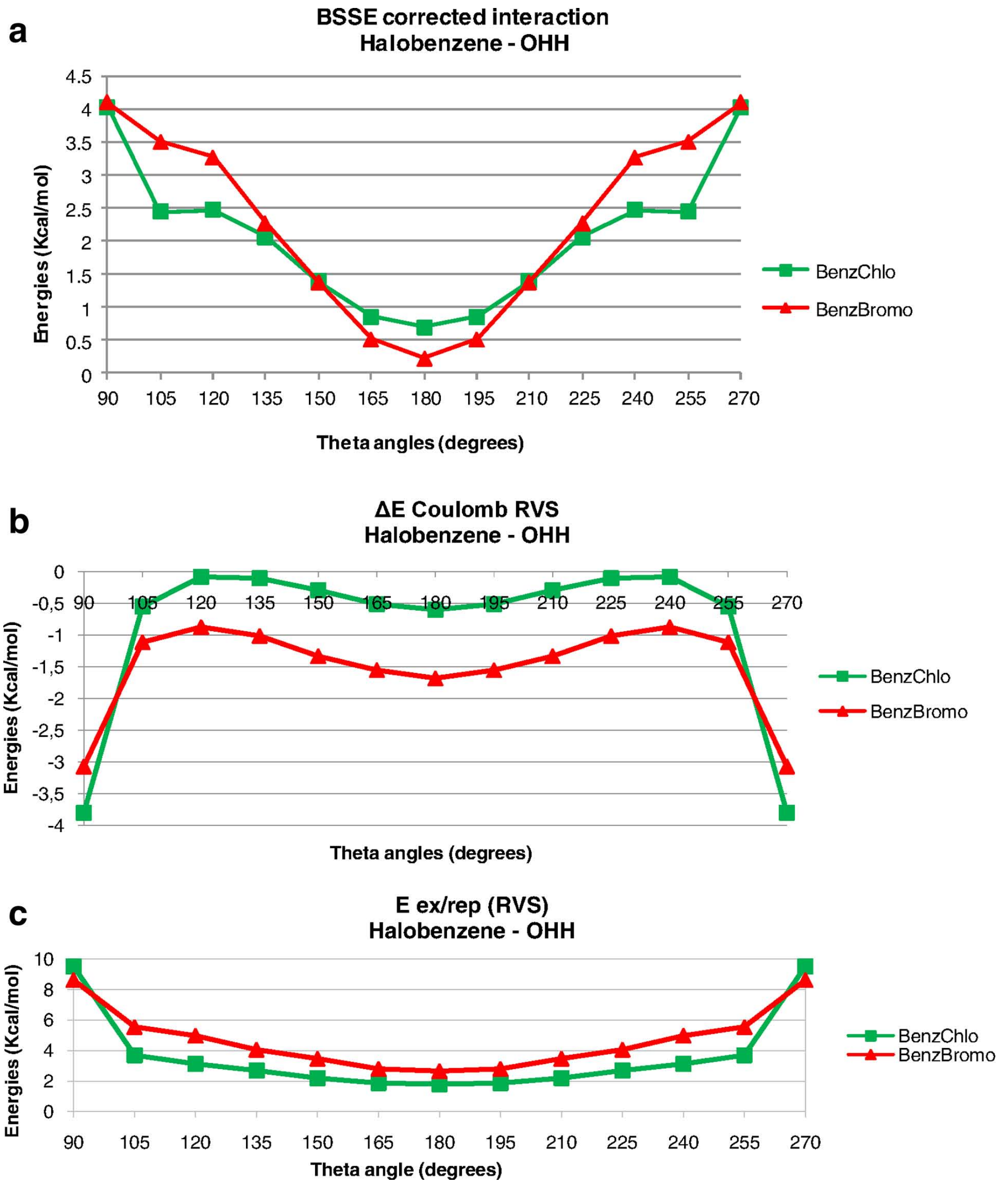

Figure 9. a–c) Halobenzene–water complex. Water approach through its O atom. In-plane evolutions of a) ΔE(RVS) b) E_C, and c) E_{exch}, as a function of the θ angle. [Color figure can be viewed in the online issue, which is available at wileyonlinelibrary.com.]

fluoro-, chloro-, and bromobenzene with a divalent cation, Mg(II), chosen so as to magnify the impact of electrostatics. Both the angularity and the magnitudes of E_{MTP} closely matched those of E_C from the RVS analysis. For X = Cl and Br, the preference for in-plane θ values at 75–90° and 255–270° is governed by the charge–quadrupole component of E_{MTP}. For X = F, the shallow angular behavior of E_{MTP} was found to result from starkly opposed trends of charge–quadrupole, disfavoring θ = 180°, and charge–charge favoring it, and not from a weaker charge–quadrupole term than with X = Cl and X = Br. In contrast to the in-plane variations, the preferences for out-of-plane locations of the probe stemmed from the charge–charge term favoring ϕ = 90° and 270° and overcoming the preference of charge–quadrupole for ϕ = 0°. With an incoming water probe interacting through one H atom, the trends were found to reflect those with the Mg(II) probe, but the amplitudes of variations were considerably damped. We have also probed the electron-depleted zones of chloro- and bromobenzene with water incoming through its O atom. The energy minimum now occurs at θ = 180°, a value which corresponded to an energy maximum upon water approach through its H atom. Again, both E_{MTP} and E_{rep} reflected the values and the trends of their RVS counterparts. Resorting to an off-centered partial charge prolonging the CX bond could possibly reproduce the interaction energies upon binding along this bond,[10] namely for θ values close to 180°.

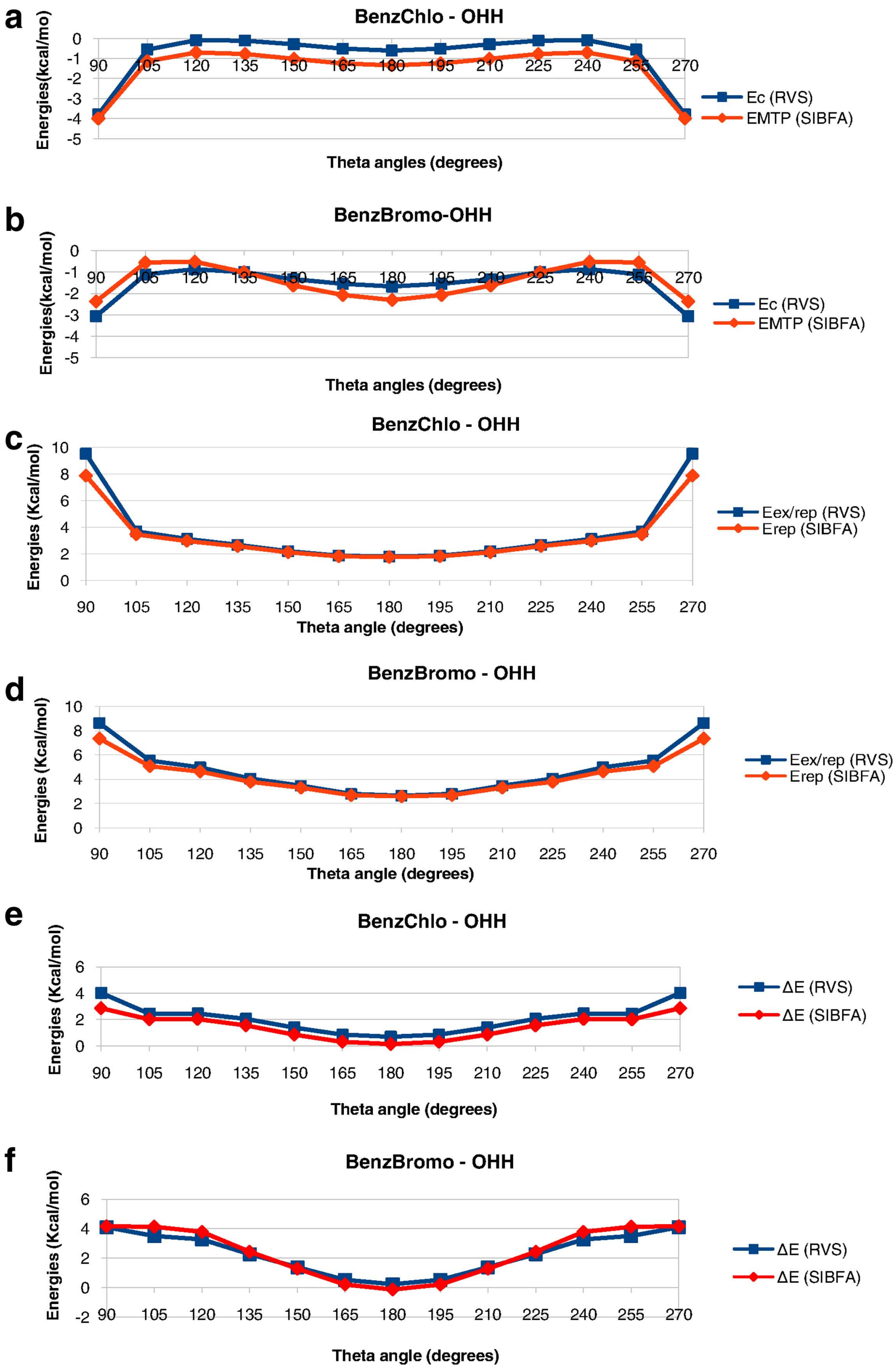

Figure 10. a–f) Halobenzene–water complex. Water approach through its O atom. Compared in-plane evolutions as a function of the θ angle of E_C(RVS) and E_{MTP} for a) chlorobenzene and b) bromobenzene, of E_{exch} and E_{rep} for c) chlorobenzene and d) bromobenzene, and of Δ*E*(RVS) and ΔE(SIBFA) for e) chlorobenzene and f) bromobenzene. [Color figure can be viewed in the online issue, which is available at wileyonlinelibrary.com.]

However, it is unlikely to reproduce equally well such interactions in the electron-rich areas, taking place for smaller in- and out-of-plane values of *θ*. Such interactions should not be bypassed upon exploring by MM or MD approaches the binding of halogenated drugs to protein or DNA targets.

Selective halogenation of aromatic rings could significantly enhance the binding affinities of ligands to their protein or nucleic targets.[1] The present results demonstrate that anisotropic, polarizable molecular mechanics (APMM) procedures enable to successfully probe both the electron-rich and electron-depleted zones which encompass and surround the CX bond. They should prompt APMM applications to a diversity of protein targets, which include kinases, the HIV-1 integrase, and Zn-metalloproteins.

Acknowledgments

We wish to sincerely thank the Association Philippe Jabre (Beirut, Lebanon) for funding the PhD research of Krystel El Hage. We also thank Dr. Mike Devereux (Department of Chemistry, University of Basel, Switzerland) for providing us with his software programs to convert the distributed Stone multipoles from G09 and the Garmer–Stevens polarizabilities from GAMESS into a form amenable to SIBFA computations. Jean-Philip Piquemal and Nohad Gresh wish to dedicate this article to the memory of the late Dr. Claude Giessner-Prettre, who deceased in March 2012.

Keywords: sigma hole · quantum chemistry · anisotropic molecular mechanics

How to cite this article: K. E. Hage, J.-P. Piquemal, Z. Hobaika, R. G. Maroun, N. Gresh, *J. Comput. Chem.* **2013,** *34,* 1125–1135. DOI: 10.1002/jcc.23242

[1] Y. Lu, Y. Wang, H. Yang, X. Yan, X. Luo, H. Jiang, W. Zhu, *J. Med. Chem.* **2000**, *52,* 2854.

[2] M. Z. Hernandes, S. M. Cavalcanti, D. R. Moreira, W. F. de Azevedo Junior, A. C. Leite, *Curr Drug Targets.* **2010**, *11,* 303.

[3] H. Matter, M. Nazaré, S. Güssregen, D. W. Will, H. Schreuder, A. Bauer, M. Urmann, K. Ritter, M. Wagner, V. Wehner, *Angew Chem Int Ed Engl.* **2009**, *48,* 2911.

[4] (a) J. P. M. Lommerse, A. J. Stone, R. Taylor, F. H. Allen, *J. Am. Chem. Soc.* **1996**, *118,* 3108; (b) P. Auffinger, F. A. Hay, E. Westhof, P. S. Ho, *Proc. Natl. Acad. Sci.* **2004**, *101,* 16789.

[5] L. A. Hardegger, B. Kuhn, B. Spinnler, L. Anselm, R. Ecabert, M. Stihle, B. Gsell, R. Thoma, J. Diez, J. Benz, J.-M. Plancher, G. Hartmann, D. W. Banner, W. Haap, F. Diederich, *Angew. Chem. Int. Ed.* **2011**, *50,* 314.

[6] K. E. Riley, P. Hobza, *Cryst. Growth. Des.* **2011**, *11,* 4272.

[7] (a) P. Metrangolo, H. Neukirch, T. Pilati, G. Resnati, *Acc. Chem. Res.* **2005**, *38,* 386; (b) P. Metrangolo, F. Meyer, T. Pilati, G. Resnati, G. Terraneo, *Angewandte Chem.* **2008**, *47,* 6114.

[8] (a) T. Clark, M. Hennemann, J. S. Murray, P. Politzer, *J. Mol. Mod.* **2007**, *13,* 291; (b) J. S. Murray, P. Lane, P. Politzer *J. Mol. Mod.* **2009**, *15,* 723; (c) P. Politzer, J. S. Murray, T. Clark, *Phys. Chem. Chem. Phys.* **2010**, *12,* 7748.

[9] (a) K. E. Riley, P. Hobza, *J. Chem. Theory Comput.* **2008**, *4,* 232, (b) K. E. Riley, J. S. Murray, P. Politzer, M. C. Concha, P. Hobza, *J. Chem. Theory Comput.* **2009**, *5,* 155; (c) J. Rezak, K. E. Riley, P. Hobza, *J. Chem. Theory Comput.* **2012**, *8,* 141; (d) M. Palusiak, *J. Mol. Struct. (THEOCHEM).* **2010**, *945,* 89; (e) P. Romaniellllo, F. Lelj, *J. Phys. Chem. A.* **2002**, *106,* 9114.

[10] (a) M. A. Ibrahim, *J. Comput. Chem.* **2011**, *32,* 2564; (b) W. L. Jorgensen, P. Schyman, *J. Chem. Theory Comput.* **2012**, DOI: 10.1021/ct300180w; (c) M. Kolar, P. Hobza, *J. Chem. Theory. Comput.* **2012**, *8(4),* 1325–1333.

[11] (a) N. Gresh, *J. Comput. Chem.* **1995**, *16,* 856; (b) N. Gresh, *Curr. Pharm. Des.* **2006**, *12,* 2121; (c) N. Gresh, G. A. Cisneros, T. A. Darden, J. Piquemal, *J. Chem. Theory. Comput.* **2007**, *3,* 1960.

[12] B. de Courcy, J.-P. Piquemal, C. Garbay, N. Gresh, *J. Am. Chem. Soc.* **2010**, *132,* 3312.

[13] (a) J. Antony, N. Gresh, L. Olsen, L. Hemmingsen, C. Schofield, R. Bauer, *J. Comput. Chem.* **2002**, *23,* 1281; (b) J. Antony, J.-P. Piquemal, N. Gresh, *J. Comput. Chem.* **2005**, *26,* 1131; (c) C. Roux, N. Gresh, L. E. Perera, J.-P. Piquemal, L. Salmon, *J. Comput. Chem.* **2007**, *28,* 938; (d) L. M. Miller Jenkins, T. Hara, S. R. Durell, R. Hayashi, J. K. Inman, J.-P. Piquemal, N. Gresh, E. Appella, *J. Am. Chem. Soc.* **2007**, *129,* 11067; (e) N. Gresh, B. de Courcy, J. P. Piquemal, J. Foret, S. Courtiol-Legourd, L. A. Salmon, *J. Phys. Chem. B.* **2011**, *115,* 8304.

[14] (a) T. H. Dunning, *J. Chem. Phys.* **1989**, *90,* 1007; (b) D. Feller, *J. Comput. Chem.* **1996**, *17,* 1571.

[15] K. L. Schuchardt, B. T. Didier, T. Elsethagen, L. Sun, V. Gurumoorthi, J. Chase, J. Li, T. L. Windus, *J. Chem. Inf. Model.* **2007**, *47,* 1045.

[16] W. J. Stevens, W. Fink, *Chem. Phys. Letts.* **1987**, *139,* 15.

[17] M. W. Schmidt, K. K. Baldridge, J. A. Boatz, S. T. Elbert, M. S. Gordon, J. H. Jensen, S. Koseki, N. Matsunaga, K. A. Nguyen, S. Su, T. L. Windus, M. Dupuis, J. A. Montgomery, *J. Comput. Chem.* **1993**, *14,* 1347.

[18] M. J. Frisch, G. W. Trucks, H. B. Schlegel, G. E. Scuseria, M. A. Robb, J. R. Cheeseman, G. Scalmani, V. Barone, B. Mennucci, G. A. Petersson, H. Nakatsuji, M. Caricato, X. Li, H. P. Hratchian, A. F. Izmaylov, J. Bloino, G. Zheng, J. L. Sonnenberg, M. Hada, M. Ehara, K. Toyota, R. Fukuda, J. Hasegawa, M. Ishida, T. Nakajima, Y. Honda, O. Kitao, H. Nakai, T. Vreven, J. A. Montgomery, Jr., J. E. Peralta, F. Ogliaro, M. Bearpark, J. J. Heyd, E. Brothers, K. N. Kudin, V. N. Staroverov, R. Kobayashi, J. Normand, K. Raghavachari, A. Rendell, J. C. Burant, S. S. Iyengar, J. Tomasi, M. Cossi, N. Rega, N. J. Millam, M. Klene, J. E. Knox, J. B. Cross, V. Bakken, C. Adamo, J. Jaramillo, R. Gomperts, R. E. Stratmann, O. Yazyev, A. J. Austin, R. Cammi, C. Pomelli, J. W. Ochterski, R. L. Martin, K. Morokuma, V. G. Zakrzewski, G. A. Voth, P. Salvador, J. J. Dannenberg, S. Dapprich, A. D. Daniels, Ö. Farkas, J. B. Foresman, J. V. Ortiz, J. Cioslowski, D. J. Fox, Gaussian 09, Revision A.1, Gaussian Inc.: Wallingford, CT, **2009**.

[19] (a) A. J. Stone, *Chem. Phys. Letts.* **1981**, *83,* 233; (b) A. J. Stone, M. Alderton, *Mol. Phys.* **1985**, *56,* 1047.

[20] (a) F. Vigné-Maeder, P. Claverie, *J. Chem Phys.* **1988**, *88,* 4934; (b) M. Dreyfus, PhD Thesis, University of Paris, **1970**; (c) P. Claverie, Thesis, Paris, **1973**, CNRS library number A.O. 8214.

[21] D. R. Garmer, W. J. Stevens, *J. Phys. Chem. A.* **1989**, *93,* 8263.

[22] (a) C. Fonseca Guerra, F. M. Bickelhaupt, J. G. Snijders, E. J. Baerends, *J. Am. Chem. Soc.* **2000**, *122,* 4117; (b) C. Fonseca Guerra, F. M. Bickelhaupt, J. G. Snijders, E. J. Baerends, *Chem. Eur. J.* **1999**, *5,* 3581; (c) J. P. Piquemal, A. Marquez, O. Parisel, C. Giessner-Prettre, *J. Comput. Chem.* **2005**, *26,* 1052.

[23] (a) E. R. Johnson, S. Keinan, P. Mori-Sanchez, J. Contreras-Garcia, A. J. Cohen, W. T. Yang, *J. Am. Chem. Soc.* **2010**, *132,* 6498; (b) J. Contreras-Garcia, E. R. Johnson, S. Keinan, R. Chaudret, J.-P. Piquemal, D. Beratan, W. Yang, *J. Chem. Theory. Comput.* **2011**, *7,* 625.

[24] N. Gresh, P. Claverie, A. Pullman, *Int. J. Quantum Chem.* **1982**, *22,* 199.

[25] S. Grimme, *J. Comput. Chem.* **2006**, *27,* 1787.

[26] M. Hennemann, J. S. Murray, P. Politzer, K. E. Riley, T. Clark, *J. Mol. Model.* **2012**, *18,* 2461.

Received: 14 November 2012
Revised: 28 December 2012
Accepted: 12 January 2013